Biodegradable Polyurethanes: Comparative Study of Electrospun Scaffolds and Films

Pablo C. Caracciolo,[1] Fabián Buffa,[1] Vinoy Thomas,[2] Yogesh K. Vohra,[2] Gustavo A. Abraham[1]

[1]*Instituto de Investigaciones en Ciencia y Tecnología de Materiales, Universidad Nacional de Mar del Plata/Consejo Nacional de Investigaciones Científicas y Técnicas, Avenida J. B. Justo 4302, B7608FDQ Mar del Plata, Argentina*
[2]*Center for Nanoscale Materials and Biointegration, Department of Physics, University of Alabama at Birmingham, 1300 University Boulevard, Birmingham, Alabama 35294*

Received 1 October 2010; accepted 6 December 2010
DOI 10.1002/app.33855
Published online 11 April 2011 in Wiley Online Library (wileyonlinelibrary.com).

ABSTRACT: The development of elastomeric, bioresorbable, and biocompatible segmented polyurethanes (SPUs) for use in tissue-engineering applications has attracted considerable interest in recent years. In this work, nonporous films and microfiber/nanofiber scaffolds, which were prepared from two different poly(ε-caprolactone)-based SPUs previously synthesized from 1,6-hexamethylene diisocyanate and novel chain extenders containing urea groups or an aromatic amino acid derivative, were studied. Their thermal properties were influenced by both the different chemical structures of the hard segments and the processing conditions. The mechanical properties of the scaffolds (the elastic modulus, ultimate strain, and tensile stress) were adequate for engineered soft-tissue constructs (e.g., myocardial tissue). The film samples displayed a low swelling degree (<2 wt %) in a phosphate-buffered solution at 37°C. The introduction of the amino acid derivative chain extender with hydrolyzable ester bonds contributed to greater degradation. The fibrous scaffolds exhibited higher hydrolytic stability than the films after short assay times because of their more crystalline structures and higher degrees of association by hydrogen bonding, but they also experienced higher mass losses under accelerated conditions (70°C). This suggested that the degradation rate was not constant but depended on the degradation time and the processing technique. © 2011 Wiley Periodicals, Inc. J Appl Polym Sci 121: 3292–3299, 2011

Key words: degradation; mechanical properties; nanofibers; polyurethanes; thermal properties

INTRODUCTION

The development of elastomeric, bioresorbable, and biocompatible segmented polyurethanes (SPUs) for use in tissue-engineering applications in the form of thin films or highly porous matrices has attracted considerable interest in recent years because of the increasing need for soft materials to be used as tissue–organ regeneration scaffolds for the replacement or repair of soft tissues such as cardiovascular tissue,[1–3] contractile muscle,[4,5] and knee-joint menisci.[6,7]

Although the properties of SPU and poly(urethane urea) films have been studied,[6,8–11] these materials have been infrequently used for the fabrication of electrospun nanofiber scaffolds;[12,13] this is surprising because these polymers represent a very large variety of materials with tailored properties.

The highly variable chemistry of SPUs allows the preparation of materials with controlled physicochemical, mechanical, and biodegradation properties that can be achieved through the appropriate selection of monomers and the manipulation of hard and soft contents. For example, the incorporation of urea linkages or aromatic groups into chain extenders strengthens hard-segment interactions through the bidentate hydrogen bonding of urea groups in adjacent chains or through π-bond stacking among adjacent aromatic rings, respectively.[14] The cooperative character of all interactions within the hard-segment domains determines the thermal, mechanical, and hydrolytic behavior.

Biodegradation into nontoxic components can be promoted by the use of aliphatic diisocyanates. Bioresorbable polyester soft segments such as poly (ε-caprolactone) (PCL)[8,15] are commonly used to provide hydrolytically labile soft segments, whereas chain extenders containing easily hydrolyzable linkages increase the SPU degradation rate.[9,16]

Correspondence to: P. C. Caracciolo (pcaracciolo@fi.mdp.edu.ar).

Contract grant sponsor: National Science Foundation (through the Nanotechnology and Interdisciplinary Research Team program); contract grant number: DMR-0402891 (to Y.K.V. and V.T.).
Contract grant sponsor: Consejo Nacional de Investigaciones Científicas y Técnicas (to P.C.C.).
Contract grant sponsor: Agencia Nacional de Promoción Científica y Tecnológica.
Contract grant sponsor: Universidad Nacional de Mar del Plata.

Two PCL-based SPUs with different hard-segment chemistries were synthesized from 1,6-hexamethylene diisocyanate (HDI) and novel chain extenders containing urea groups or an aromatic amino acid derivative in these laboratories for soft-tissue applications.[10] In this study, the effects of the hard-segment chemistry/composition and the processing technique (nonporous cast films and nonwoven fibrous meshes) on the thermal and mechanical properties, swelling, and *in vitro* degradation behavior of these SPUs were analyzed and compared.

EXPERIMENTAL

Materials

PCL diol (number-average molecular weight = 2250 Da), aliphatic diurea diol (A–H–A), and amino acid derivative diester diphenol (D–E–D) chain extenders and HDI-based polyurethanes were synthesized according to previously reported procedures.[10] The poly(ester urethane urea) and poly(ester urethane) samples were designated as PHH or PHD according to the chain extender used (A–H–A or D–E–D, respectively). *N*,*N*-Dimethylacetamide (DMAc) and 1,1,1,3,3,3-hexafluoro-2-propanol (HFP) were purchased from Aldrich Chemical Co.

Preparation of the films and scaffolds

Nonporous films were prepared by solution casting from DMAc (10% w/v) onto siliconized Petri dishes. The solvent was evaporated at 60°C, and the films were finally dried *in vacuo* for 24 h. Microfiber/nanofiber scaffolds were obtained via the electrospinning of SPU solutions prepared by the dissolution of SPUs in HFP (20% w/v) with heating and stirring. Each of the as-prepared solutions was loaded into a standard 10-mL plastic syringe connected to a polyamide tube, the open end of which was attached to a blunt 18-gauge stainless steel hypodermic needle (i.d. = 0.838 mm), which was used as the nozzle. A programmable syringe pump (Activa A22 ADOX S.A., Ituzaingó, Argentina) that was connected to the syringe controlled the flow rate. A high-voltage power source (ES30P, Gamma High Voltage Research, Inc.) was used to charge the solution; the emitting electrode of positive polarity was attached to the nozzle, and the grounding electrode was attached to an aluminum collecting device. All experiments were carried out at room temperature in a chamber with a ventilation system. The solutions were electrospun with a positive high voltage of 15 kV, a working distance of 15 cm (the distance between the needle tip and the collecting plate), and a solution feeding rate of 0.5 (for PHD) or 3 mL/h (for PHH) in accordance with our earlier report.[17] The electrospun fibers were deposited onto the grounded, flat aluminum plate, dried *in vacuo* at room temperature to fully eliminate the residual solvent, and stored in a desiccator. The morphology of the electrospun scaffolds was examined with scanning electron microscopy (SEM; JEOL, Ltd.) at an accelerating voltage of 10 kV after gold sputtering. The fiber diameter average and the diameter distribution were obtained with an image analyzer (Image-Pro Plus, Media Cybernetics, Inc.).

Thermal and mechanical characterization

Differential scanning calorimetry (DSC) was performed with a Shimadzu DSC-50 calorimeter (Kyoto, Japan). Scans were performed at a heating rate of 10°C/min. Thermograms were obtained in the range of −100 to 250°C under a nitrogen purge. The glass-transition temperature was taken as the onset of the transition. The degree of crystallinity (X_c) of soft domains was calculated with 148.05 J/g used as the melting heat for pure high-molecular-weight PCL.[18]

Uniaxial tensile stress–strain data were obtained with an Instron model 4467 testing machine (Norwood, MA). Sample strips with dimensions of 35 mm × 5 mm × t (t = 0.4 ± 0.1 mm for polymer films and t = 1.25 ± 0.15 mm for electrospun samples) were employed. Tests were performed at room temperature (18 ± 2°C) with a crosshead speed of 5 mm/min, an extensometer for elastomers (Instron), and a loading cell of 100 N. At least four replicate measurements were taken and averaged.

Swelling and degradation behavior

The swelling and degradation of SPUs were conducted with film samples with dimensions of 1 cm × 1 cm × h (h = 0.070 ± 0.010 cm) and with electrospun samples with dimensions of 2 cm × 1 cm × h (h = 0.125 ± 0.015 cm); the resulting average mass was 0.1 g. SPU samples (n = 3) were placed in vials with 5 mL of a phosphate-buffered solution (PBS; pH 7.4) containing 0.05 wt % sodium azide as a bacteriostatic agent.

Swelling studies were carried out at 37°C for 5 h. The swollen samples were removed at predetermined time intervals, wiped gently with filter paper, and weighed. The mass change resulting from the water uptake, which was expressed as a percentage, was calculated according to the following formula:

$$\text{Water uptake } (\%) = \frac{m_t - m_o}{m_o} \times 100 \qquad (1)$$

where m_o and m_t are the masses of the dry and wet samples, respectively.

Hydrolytic degradation was carried out through the immersion of the specimens in PBS at 37°C[19] for 24 weeks. The medium was not changed during the testing period so that we could assess whether the release of degradation products caused any change in the pH of the medium. The samples were removed from the buffer at a given time, were rinsed three times with distilled water, were dried to a constant weight with anhydrous P_2O_5 *in vacuo* (for film samples) or lyophilized (for electrospun samples), and were weighed to determine the mass loss as follows:

$$\text{Mass loss } (\%) = \frac{m_o - m_t}{m_o} \times 100 \quad (2)$$

where m_o and m_t are the masses of the sample before and after testing, respectively. The pH values were determined for each degradation medium at different times.

Accelerated degradation was carried out in a hydrolytic medium (PBS) at 70°C for 40 days.

All values were calculated with a 90% confidence interval for standard deviations.

RESULTS AND DISCUSSION

SPUs

Two PCL-based SPUs, PHH and PHD, were successfully synthesized and characterized in our laboratory with the incorporation of a diisocyanate (HDI) and two novel chain extenders (A–H–A and D–E–D, respectively). The SPUs were synthesized by a two-step polymerization method. The SPU hard-segment contents were in the range of 21.8–23.6 wt %. The obtained polymers were not sticky and were slightly whitish.

A–H–A has a linear and symmetrical structure with two urea groups. Coupled with the presence of an even number of carbon atoms, this allowed a close chain association of PHH by hydrogen bonding [Fig. 1(a)], as could be seen in a Fourier transform infrared spectrum.[10] On the other hand, D–E–D also

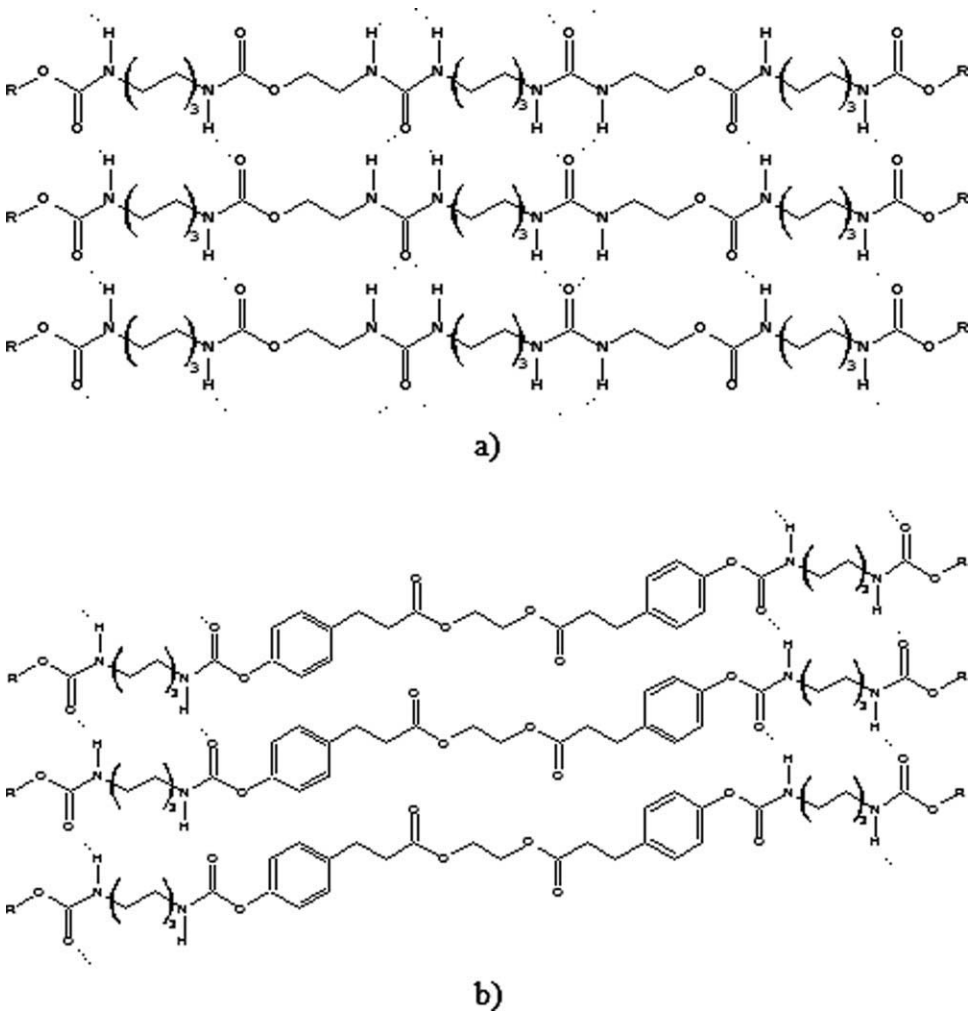

Figure 1 Proposed chemical structures for the hard segments interacting by (a) hydrogen bonding in PHH and (b) hydrogen bonding and ϕ stacking in PHD.

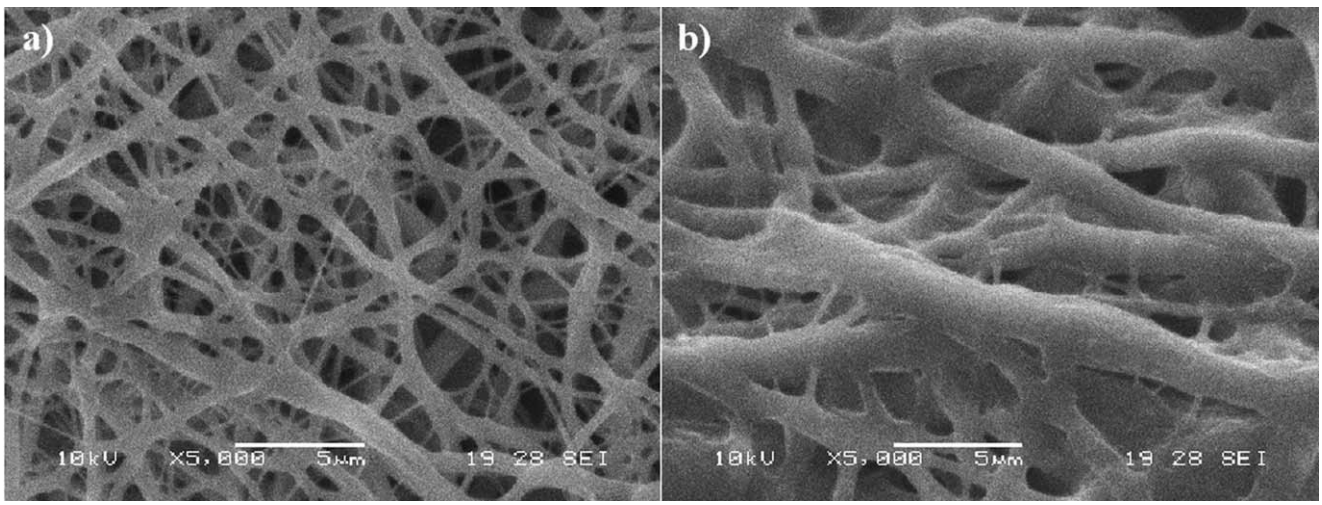

Figure 2 SEM micrographs of electrospun scaffolds: (a) PHH and (b) PHD.

has a symmetric structure and two aromatic rings, which led to a chain association of PHD by π stacking [Fig. 1(b)]. Urethane linkages, which connected soft and hard segments, also allowed a chain association of SPU chains by hydrogen bonding. The structure of the chain extender determined the association degree of the hard segments. Therefore, the observed viscosity of the SPUs was related to both the isocyanate and the chain-extender chemistry. Intrinsic viscosity measurements were carried out by capillary viscosimetry to characterize in a relative way the molecular weights of the polyurethanes. An Ubbelohde-type OC viscometer (Cannon State College, PA) with DMAc as a solvent was used at 30 ± 0.1°C. Intrinsic viscosities of 0.40 dL/g for PHH and 0.49 dL/g for PHD were obtained.

Electrospun scaffolds

The conditions for obtaining the porous PHH and PHD scaffolds by electrospinning were optimized in a previous study.[17] Highly polar HFP was the most adequate solvent for electrospinning the highly hydrogen-bonded materials into bead-free fibers (Fig. 2). The resulting fiber diameter averages were 0.70 ± 0.20 μm for PHH scaffolds and 1.39 ± 0.56 μm for PHD scaffolds. Both systems showed a mixed structure of microfibers connected by nanofibers, these fibers being thicker for the PHD scaffolds and leading to a more open porous structure.

Thermal properties

Figure 3 shows the DSC thermograms of the samples, whereas the thermal properties of the SPU films and scaffolds (determined in the first scan) are summarized in Table I.

In the low-temperature range, the films exhibited soft-segment glass-transition temperature ($T_{g,s}$) values slightly lower than those of the corresponding electrospun matrices. The $T_{g,s}$ value of the PHH film (PHH_{film}) was closest to the macrodiol glass-transition temperature (−69.3°C) and the lowest value found in the literature; this indicated the presence of microphases with a certain separation degree in PHH. Moreover, PHD presented higher values of $T_{g,s}$, which showed the presence of a morphology with higher phase mixing. The film thermograms displayed two endothermic peaks [i.e., soft-segment melting temperature ($T_{m,s}$) values] associated with the melting of soft domains. These $T_{m,s}$ values were lower than the macrodiol melting temperature (50.5°C), and this could be attributed to the presence of crystalline phases of lower extension and paracrystalline domains. The soft-segment melting heat ($\Delta H_{m,s}$) values showed the effect of

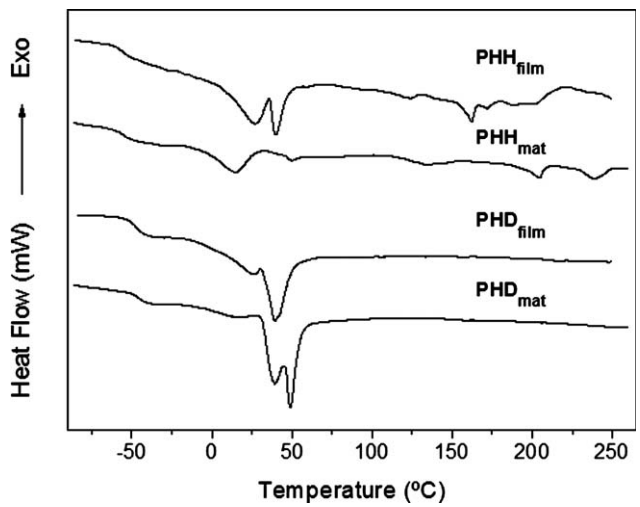

Figure 3 DSC thermograms of SPU films and scaffolds.

TABLE I
Thermal Properties of the SPU Films and Scaffolds

SPU	$T_{g,s}$ (°C)	$T_{m,s}$ (°C)	$\Delta H_{m,s}$ (J/g of SPU)	X_c (%)	$T_{g,h}$ (°C)	$T_{m,h}$ (°C)	$\Delta H_{m,h}$ (J/g of SPU)
PHH_{film}	−61.4	27.0, 39.9	31.5	27.2	108.2	162.2, 171.4	3.4
PHH_{mat}	−59.2	14.8	13.7	11.8	115.3	204.3, 238.4	9.6
PHD_{film}	−53.2	26.6, 39.3	29.8	26.4	–	–	–
PHD_{mat}	−50.4	39.5, 49.0	42.6	37.7	–	–	–

the connectivity between the soft and hard segments on crystallization. The restriction of the mobility of SPU chains produced a marked decrease in the X_c values of the soft domains (X_c for the PCL diol = 65.5%). The PHH electrospun matrix (PHH_{mat}) thermogram presented only one peak associated with the melting of soft domains; the temperature and melting heat values were lower than those obtained for PHH_{film}. The main difference depended on the crystallinity. X_c of PHH_{mat} decreased more than 50% with respect to X_c of PHH_{film}. The morphology obtained during electrospinning is governed by simultaneous processes: the evaporation of the solvent and the elongation of the solidifying fiber. In semicrystalline polymers, solidification is also related to the formation of crystals. A shorter crystallization time is expected to result in small crystallites with defects and thus lower X_c values.[20] Otherwise, solidification during film formation is slower and takes place at higher temperatures; this leads to a material with a higher X_c value. More restricted chain mobility during the rapid solidification of a material contributes to a marked decrease in X_c. The PHD electrospun matrix (PHD_{mat}) exhibited thermal behavior very different from that of PHH_{mat} and showed two peaks associated with the melting of soft domains at temperatures higher than those for the PHD film (PHD_{film}). X_c was higher for PHD_{mat} than PHD_{film}; this phenomenon is hardly found in the literature. The presence of a higher fraction of crystals with a higher degree of order is difficult to explain in terms of intermolecular interactions. Zhuo et al.[12] also observed higher crystallinity in SPU nanofibers with shape memory, and they attributed this fact to a positive tropism of the soft segment. The higher X_c values for PHD_{mat} versus PHH_{mat} could be explained by the different morphologies of the scaffolds, as mentioned before. Higher fiber diameter averages allow greater chain mobility and thus a better organized and more crystalline material. A complete understanding of this phenomenon requires further studies so that we can analyze in a more detailed way the different crystalline morphologies that evolve in bulk and microfibers, for which crystallization occurs under completely different conditions and restrictions.

In the high-temperature range, PHH_{film} exhibited a second-order transition corresponding to the hard-segment glass-transition temperature ($T_{g,h}$), which was slightly lower than that for PHH_{mat}. Two endothermic peaks were observed at higher temperatures in both cases, and they were attributed to the melting of hard domains with different degrees of order. The presence of functional groups with high cohesive energy (two urethane groups and two urea groups) in hard segments of PHH, coupled with the structural symmetry [Fig. 1(a)], promoted the phase separation. The hard-segment melting temperature ($T_{m,h}$) and hard-segment melting heat ($\Delta H_{m,h}$) values were higher for PHH_{mat}. This behavior could be associated with the influence of the elongational flow due to the processing technique, which produced higher interactions among shorter hard segments. PHD did not show thermal transitions associated with hard domains, and this could be attributed to the fact that large chain extenders make difficult the ordering that leads to the crystallization of hard segments [Fig. 1(b)]. Therefore, the composition and structure of chain extenders have significant effects on the thermal behavior and the processing method.

Although there are many studies in the literature on PCL_{2000}-based poly(ester urethane)s and poly (esterurethane urea)s, only a few have reported the presence of hard-domain thermal transitions. Some are HDI-formulated SPUs using 1,4-diamino

TABLE II
Mechanical Properties of the SPU Films and Scaffolds

SPU	Young's modulus (MPa)	Ultimate tensile stress (MPa)	Ultimate strain (%)	Yield stress (MPa)	Yield strain (%)
PHH_{film}	16 ± 4	5.1 ± 0.3	469 ± 38	–	–
PHH_{mat}	0.5 ± 0.01	0.4 ± 0.02	124 ± 3.2	–	–
PHD_{film}	54 ± 4	6.9 ± 1.5	1006 ± 120	3.4 ± 0.9	19 ± 6
PHD_{mat}	7.5 ± 0.1	0.7 ± 0.01	54 ± 1.1	–	–

butane[11] or a phenylalanine derivative[9] as a chain extender. As far as we know, to date, PHH has resulted in the only HDI-formulated SPU showing a $T_{g,h}$ value and high $T_{m,h}$ values.

Mechanical properties

The mechanical properties of the SPU films and scaffolds, as determined by uniaxial tensile stress–strain testing, are shown in Table II. The values of the ultimate tensile stress, ultimate strain, yield stress, yield strain, and Young's modulus are listed for these samples.

Figure 4 shows the stress–strain curves for the SPU samples. Two different behaviors were found for the films. On the one hand, PHH_{film} behaved as a soft elastomer and had lower ultimate properties and Young's modulus values than PHD_{film}. Additionally, the stress increased with the strain until the chains became aligned and reached their maximum extension before breaking. There was no drawing of the polymer or whitening due to strain-induced crystallization during tests. It is evident that the chemical structure and symmetry of HDI and the A–H–A chain extender enhanced the secondary bonding in PHH_{film}: the molecular chains are closely packed and parallel, and this increases the ability of the hard segment to act as a physical crosslinking site [Fig. 1(a)]. On the other hand, PHD had a different hard-segment structure [Fig. 1(b)] and behaved as a tough plastic. This polymer displayed a yield point followed by a necking region in which a very extensive reorganization of the polymer took place. Once the yielding was passed, the stress dropped to a slightly lower value, and then PHD_{film} exhibited plastic deformation by cold drawing with increasing stress. At this point, necking advanced through the entire specimen. At the end of this reorganization, the stress continued to increase with strain until failure occurred. PHD_{film} displayed a higher ultimate strain than PHH_{film} (Table II). The combination of a high tensile strength and a high strain at break for PHD_{film} gave rise to an increase in the toughness, as determined by the area under the curve. In this case, the symmetric structures of HDI and the D–E–D chain extender enhanced the secondary bonding within the hard segment [Fig. 1(b)] by hydrogen-bonding and π-stacking interactions, respectively.

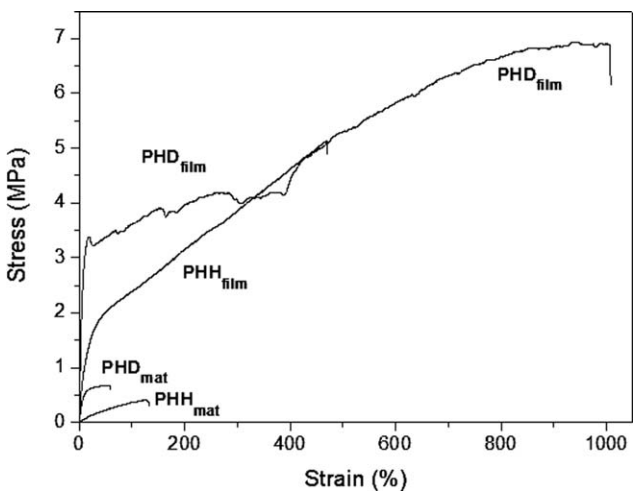

Figure 4 Representative tensile stress–strain curves for SPU films and scaffolds.

The fibrous scaffolds displayed increasing stress with strain during the whole test before breaking. There was no drawing of the polymers (Fig. 4). The different crystallinities of PHD_{mat} and PHH_{mat} were reflected by the stiffness of the materials (Table II). PHD_{mat} exhibited a Young's modulus 15 times higher than that shown by PHH_{mat}. An ultimate strain that was 50% lower for PHD_{mat} was due to the presence of higher average diameter fibers, which led to a more open porous structure in comparison with PHH_{film}. The crystalline morphology adopted by the scaffolds, the product of the processing method, and the chemical structure of the hard segment highly influenced the mechanical properties. The mechanical properties of the highly porous scaffolds were lower than those obtained for the films. Although very few studies have examined the mechanical properties of polyurethane scaffolds, this behavior agrees with that reported in the literature.[21] The capacity for reinforcement of the crystalline domains in a fibrous structure is lower, and the presence of defects leads to a lower ultimate strain.

For the regeneration of myocardial tissue, soft elastomeric materials are required; according to theoretical simulations, the value of the elastic modulus must be between tens of kilopascals and approximately 1 MPa.[22] The elastomeric nature required for these cyclic-loading applications is impossible to achieve with traditional polyesters. In particular, electrospun PHH_{mat} has a low elastic modulus and could be a candidate for the design of cardiac patches along with the seeding of cardiomyocytes, which restore the functionality of infarcted tissue regions. Simultaneous electrospraying of cells and electrospinning of poly(urethane urea) fibers for the fabrication of cell-microintegrated scaffolds have been reported.[5]

Swelling and degradation characteristics

Swelling behavior

The films displayed similar swelling behavior and a low degree of swelling (<2%; Table III), which was consistent with a high concentration of PCL. The water uptake took place mainly in the first 2 h; the increase after that was not appreciable. Otherwise, the scaffolds showed rapid water absorption that

TABLE III
Swelling, Hydrolytic, and Accelerated Hydrolytic Behavior of the SPU Films and Scaffolds

SPU	Water uptake (%)	Mass loss at 24 weeks (%)	pH at 24 weeks	Mass loss at 40 days and 70°C (%)	pH at 40 days and 70°C
PHH_{film}	1.45 ± 0.13	1.97 ± 0.13	7.28 ± 0.02	16.84 ± 1.08	6.05 ± 0.25
PHH_{mat}	175.74 ± 20.07	1.05 ± 0.15	7.32 ± 0.02	21.43 ± 1.24	5.71 ± 0.31
PHD_{film}	1.48 ± 0.16	3.20 ± 0.18	7.19 ± 0.01	17.55 ± 0.67	5.94 ± 0.10
PHD_{mat}	113.63 ± 12.36	3.79 ± 0.24	7.14 ± 0.02	Fragmented	4.95 ± 0.35

remained constant after 10 min of soaking in PBS. These values were much higher than the film values, and the rapid absorption indicated that the water was mainly introduced into the interconnected pores of the matrices.

Hydrolytic degradation

The hydrolytic degradation media of the films and scaffolds showed slight decreases in the pH after 24 weeks of degradation, the pH change being less than 0.30 in all cases (Table III). This fall in the pH values could be attributed to the release of degradation products with carboxylic acid groups, such as ε-hydroxycaproic acid.

Figure 5 shows the hydrolytic behavior of the SPU films and scaffolds at 37°C. The samples exhibited mass-loss values below 4% after a 24-week assay (Table III). PHD presented higher degradation values than PHH in both scaffold and film samples. The difference between these two materials depended on the chemical structure of the chain extender. D–E–D contains two hydrolyzable ester groups; these were incorporated into the hard segments of PHD, acted as degradation sites, and contributed to the observed behavior.

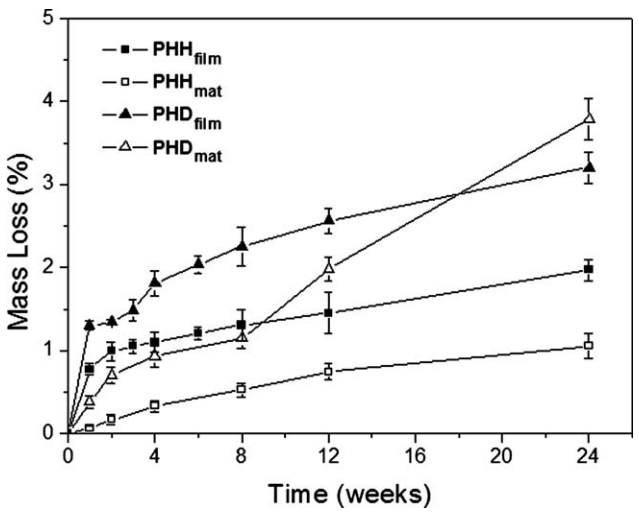

Figure 5 Hydrolytic behavior of the SPU films and scaffolds at 37°C in PBS.

Surprisingly, PHH_{mat} showed lower mass-loss values than PHH_{film} for the assayed degradation time. Despite its fibrous structure, which provided easier access for water into the matrix (evidenced by its much higher water absorption), PHH_{mat} showed mass-loss values that were 50% lower than those for PHH_{film} after 24 weeks in PBS. These results can be explained by the different hard-domain crystallinity degrees of the fibrous and compact SPU structures. More crystalline structures and greater degrees of chain association by hydrogen bonding hindered the entry of water into the materials to a higher extent, so they degraded at a lower rate.

PHD_{mat} also showed lower degradation rates than PHD_{film} for short degradation times, probably because of its higher soft-domain crystallinity. However, after 8 weeks, the degradation rate of PHD_{mat} increased considerably, the mass loss of PHD_{mat} being higher than the mass loss of PHD_{film} after 24 weeks in PBS. It is possible that the fibrous structure of PHD became the main factor controlling the degradation rate for this assay time.

Despite the higher X_c values and the lower water-uptake values of PHD_{mat} with respect to PHH_{mat}, its mass loss was higher. As mentioned before, the presence of a chain extender containing hydrolyzable ester groups contributed to the degradation behavior.

Accelerated behavior

Table III shows the degradation results under accelerated hydrolytic conditions for the films and scaffolds. The mass-loss values for the scaffolds were higher than those obtained for the films. PHD_{mat} showed partial dissolution with a residue lacking mechanical strength. These results agree with the hydrolytic behavior found for PHD and suggest that PHH behaved in the same way with longer degradation times. Thus, the degradation rate seemed to be not constant but dependent on the degradation time and the type of sample. The scaffolds initially degraded more slowly than the films, but then their rate increased more. The pH values indicate that the degradation process was

autocatalyzed by the acidic media due to the degradation products.

CONCLUSIONS

Both the different chemical structures of the hard segments and the processing conditions influenced the phase separation of the SPUs into soft and hard domains, as evidenced by the thermal behavior of the materials. The crystalline morphology of the microfibers/nanofibers occurred under conditions completely different from those for the films, and this made a comparative analysis complex.

The mechanical behavior of the scaffolds depended on their adopted crystalline structure, which was determined by the experimental processing conditions and the chemical structure of the hard segments.

The chemical structure of the chain extenders had a significant impact on the hydrolytic stability of the SPUs. The introduction of a chain extender with ester bonds added hydrolyzable sites to the hard segments, which contributed to the greater degradation of PHD. The fibrous morphology of the scaffolds influenced the water absorption and hydrolytic degradation rate. More crystalline structures and higher degrees of association by hydrogen bonding hindered the entry of water into the material to a greater extent, so the initial degradation was less rapid. Otherwise, the higher mass-loss values of the scaffolds versus the films under the accelerated hydrolytic conditions indicated that the degradation rate was not constant but depended on the degradation time and the type of sample. The fibrous structure became the main factor controlling the degradation rate for long degradation times.

The obtained scaffolds, which have highly porous structures and interconnected pores and degrade into nontoxic products, are suitable for biomedical applications such as soft-tissue engineering and controlled-drug release.

References

1. Alperin, C.; Zandstra, P. W.; Woodhouse, K. A. Biomaterials 2005, 35, 7377.
2. Fujimoto, K. L.; Guan, J.; Oshima, H.; Sakai, T.; Wagner, W. R. Thorac Surg 2007, 83, 648.
3. Guan, J.; Fujimoto, K. L.; Sacks, M. S.; Wagner, W. R. Biomaterials 2005, 26, 3961.
4. Riboldi, S. A.; Sadr, N.; Pigini, L.; Neuenschwander, P.; Simonet, M.; Mognol, P.; Sampaolesi, M.; Cossu, G.; Mantero, S. J Biomed Mater Res Part A 2008, 84, 1094.
5. Stankus, J. J.; Guan, J.; Fujimoto, K.; Wagner, W. R. Biomaterials 2006, 27, 735.
6. Heijkants, R. G. J. C.; van Calck, R. V.; van Tienen, T. G.; de Groot, J. H.; Buma, P.; Pennings, A. J.; Veth, R. P. H.; Schouten, A. J. Biomaterials 2005, 26, 4219.
7. Spaans, C. J.; de Groot, J. H.; Dekens, F. G.; Pennings, A. J. Polym Bull 1998, 41, 131.
8. Guan, J. J.; Sacks, M. S.; Beckman, E. J.; Wagner, W. R. J Biomed Mater Res Part A 2002, 61, 493.
9. Skarja, G. A.; Woodhouse, K. A. J Biomater Sci Polym Ed 1998, 9, 271.
10. Caracciolo, P. C.; Buffa, F.; Abraham, G. A. J Mater Sci: Mater Med 2009, 20, 145.
11. de Groot, J. H.; de Vrijer, R.; Wildeboer, B. S.; Spaans, C. J.; Pennings, A. J. Polym Bull 1997, 38, 211.
12. Zhuo, H.; Hu, J.; Chen, S. Mater Lett 2008, 62, 2074.
13. Demir, R. R.; Yilgor, I.; Yilgor, E.; Erman, B. Polymer 2002, 43, 3303.
14. Dieterich, D.; Grigat, E.; Hahn, W. In Polyurethane Handbook; Oertel, G., Ed.; Hanser: Munich, 1985; p 34.
15. Cohn, D.; Stern, T.; Gonzales, M. F.; Epstein, J. J Biomed Mater Res Part A 2002, 59, 273.
16. Moore, T. Ph.D. Thesis, Swinburne University of Technology, 2005.
17. Caracciolo, P. C.; Thomas, V.; Vohra, Y. K.; Buffa, F.; Abraham, G. A. J Mater Sci: Mater Med 2009, 20, 2129.
18. Properties of Polymers, 4th ed.; Van Krevelen, D. W., te Nijenhuis, K., Eds.; Elsevier: Amsterdam, The Netherlands, 2009; p 121.
19. Zhang, X.; Thomas, V.; Vohra, Y. K. J Biomed Mater Res Appl Biomater 2009, 89, 135.
20. Dhanalakshmi, M.; Jog, J. P. eXPRESS Polym Lett 2008, 2, 540.
21. Stankus, J. J.; Guan, J.; Wagner, W. R. J Biomed Mater Res Part A 2004, 70, 603.
22. Chen, Q. Z.; Bismarck, A.; Hansen, U.; Junaid, S.; Tran, M. Q.; Harding, S. E.; Ali, N. N.; Boccaccini, A. R. Biomaterials 2008, 29, 47.